JACS
JOURNAL OF THE AMERICAN CHEMICAL SOCIETY
Communication
pubs.acs.org/JACS

Sc^{3+}-Triggered Oxoiron(IV) Formation from O_2 and its Non-Heme Iron(II) Precursor via a Sc^{3+}–Peroxo–Fe^{3+} Intermediate

Feifei Li,[†,§] Katherine M. Van Heuvelen,[†,∥] Katlyn K. Meier,[‡] Eckard Münck,*[,‡] and Lawrence Que, Jr.*[,†]

[†]Department of Chemistry and Center for Metals in Biocatalysis, University of Minnesota, Minneapolis, Minnesota 55455, United States

[‡]Department of Chemistry, Carnegie Mellon University, Pittsburgh, Pennsylvania 15213, United States

Supporting Information

ABSTRACT: We report that redox-inactive Sc^{3+} can trigger O_2 activation by the Fe^{II}(TMC) center (TMC = tetramethylcyclam) to generate the corresponding oxoiron(IV) complex in the presence of BPh_4^- as an electron donor. To model a possible intermediate in the above reaction, we generated an unprecedented Sc^{3+} adduct of $[Fe^{III}(\eta^2\text{-}O_2)(TMC)]^+$ by an alternative route, which was found to have an Fe^{3+}–(μ-η^2:η^2-peroxo)–Sc^{3+} core and to convert to the oxoiron(IV) complex. These results have important implications for the role a Lewis acid can play in facilitating O–O bond cleavage during the course of O_2 activation at non-heme iron centers.

There is much current interest in investigating the ability of redox-inactive metal ions to modulate redox reactions by virtue of their Lewis acidity, particularly with respect to their possible roles in O_2 evolution[1] and activation.[2,3] For example, the oxygen-evolving complex of Photosystem II requires a redox-inactive Ca^{2+} ion to produce O_2.[1] In addition, redox-inactive ions have been found to affect the stabilities and reactivities of high-valent metal–oxo complexes in biomimetic systems[2] and to accelerate O_2 activation by Fe^{II} and Mn^{II} complexes.[3] In the latter case, heterobimetallic O_2 adducts and high-valent metal–oxo species are presumably involved but have not been observed. We previously demonstrated that $[Fe^{II}(TMC)(NCCH_3)]^{2+}$ (**1**) (TMC = 1,4,8,11-tetramethylcyclam) reacts with O_2 in CH_3CN in the presence of stoichiometric H^+ and BPh_4^- to form $[Fe^{IV}O(TMC)(NCCH_3)]^{2+}$ (**4**).[4] Herein we report that a redox-inactive Sc^{3+} ion can replace the strong acid in this reaction to *trigger* the formation of **4**. An unprecedented Sc^{3+} adduct (**3**) of $[Fe^{III}(\eta^2\text{-}O_2)(TMC)]^+$ (**2**) was trapped by an alternative route, spectroscopically characterized, and found to convert to **4** (Scheme 1).

Complex **1** is air-stable in acetonitrile solution for days. However, the addition of 1 equiv of $Sc(OTf)_3$ together with 1 equiv of $NaBPh_4$ to an aerobic solution of **1** resulted in the formation of **4** in >70% yield over the course of ∼1 h at 0 °C, as indicated by its signature near-IR band at 820 nm (Figure 1A).[5] Electrospray ionization mass spectrometry (ESI-MS) analysis of the solution revealed the evolution of a prominent peak at m/z 477.0 that was assigned to the $\{[Fe^{IV}(O)(TMC)](OTf)\}^+$ ion on the basis of its position and isotope distribution pattern [Figure S1 in the Supporting Information (SI)]. When the reaction was carried out with $^{18}O_2$, the m/z 477 peak showed an upshift of 2 units (Figure S2), confirming that the oxo moiety of **4** was derived from O_2 *and* that O–O bond cleavage must occur for the formation of **4** from **1** and O_2.

Scheme 1. Proposed Mechanism for the Formation of 4 from 1 and O_2

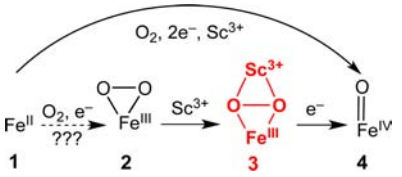

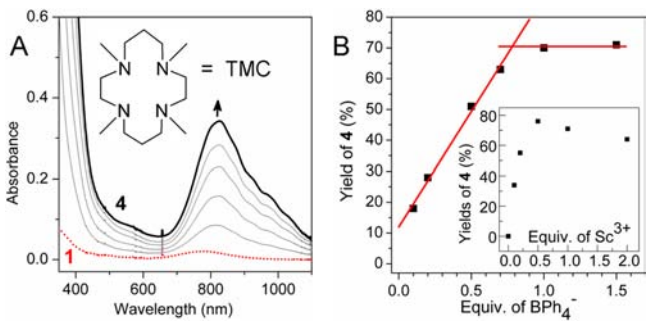

Figure 1. Reaction of 0.96 mM **1** with $NaBPh_4$ and $Sc(OTf)_3$ in aerobic CH_3CN at 0 °C. (A) UV–vis spectral changes observed with 1 equiv of $NaBPh_4$ and 1 equiv of $Sc(OTf)_3$. Inset: structure of the TMC ligand. (B) Plot of the yield of **4** vs equivalents of BPh_4^- in the presence of 1 equiv of Sc^{3+}. Inset: plot of the yield of **4** vs equivalents of Sc^{3+} with 1 equiv of BPh_4^-.

Further investigation demonstrated that both Sc^{3+} and BPh_4^- are required for the formation of **4** from **1**, as addition of either BPh_4^- or Sc^{3+} alone to **1** in air-saturated CH_3CN solution did not elicit any detectable change in the UV–vis spectrum. In addition, the yield of **4** was linearly correlated with the amount of BPh_4^- added, plateauing at 1.0 equiv of BPh_4^- (Figure 1B). ^1H NMR studies of the final solution showed that BPh_4^- had decomposed to give 1,1′-biphenyl (Figure S3) with a stoichiometry of 0.95 ± 0.15 equiv relative to **1**, demonstrating that BPh_4^- provides the two electrons needed to convert **1** and O_2 into **4**. On the other hand, a substoichiometric amount of

Received: March 14, 2013
Published: June 26, 2013

   dx.doi.org/10.1021/ja402645y | J. Am. Chem. Soc. 2013, 135, 10198–10201

Sc^{3+} was sufficient for the maximal formation of **4** (Figure 1B inset), suggesting that Sc^{3+} can act somewhat "catalytically".

As shown in Figure 1A, no intermediates were evident in the UV−vis spectra during the conversion of **1** to **4**.[6] To account for the role of Sc^{3+} in this transformation, we propose the formation of a Sc^{3+}−peroxo−Fe^{3+} adduct that is reminiscent of the Fe^{III}−OOH species proposed in the H^+ and BPh_4^--promoted generation of **4** from O_2 and **1**.[4,7] To test this hypothesis, $Sc(OTf)_3$ was added to a solution of the blue $Fe^{III}(\eta^2\text{-}O_2)$ complex **2** (purified via precipitation as its BPh_4 salt; see the SI for details), which resulted in the immediate generation of a magenta intermediate, **3**, and its subsequent conversion to **4** in ∼70% yield over the course of ∼1 h at −10 °C (Figure 2A).

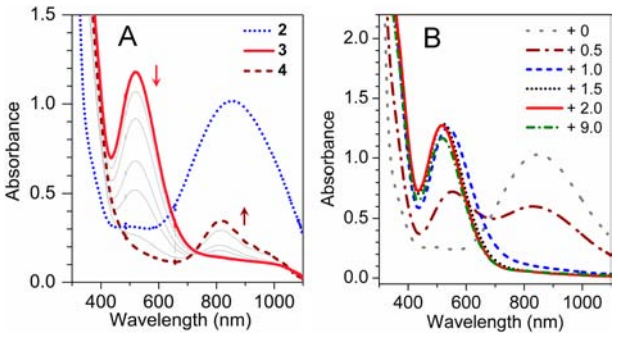

Figure 2. (A) UV−vis spectral changes upon addition of 3 equiv of Sc^{3+} to 1.5 mM *purified* **2** (ε_{835} = 650 M^{-1} cm^{-1}) in CH_3CN at −10 °C, instantly generating **3** (ε_{520} = 780 M^{-1} cm^{-1}), which in turn decayed to **4**. (B) UV−vis changes upon titration of 1.5 mM **2** with Sc^{3+} (0, 0.5, 1.0, 1.5, 2.0, and 9.0 equiv) in CH_3CN at −40 °C.

What is the identity of complex **3**? It exhibits a λ_{max} of 520 nm (ε_{520} = 780 M^{-1} cm^{-1}), as established from its UV−vis spectrum (Figure 2A) and Mössbauer analysis. The large blue shift observed for the peroxo → Fe(III) charge-transfer band of **2** (λ_{max} = 835 nm) is reminiscent of that seen upon protonation of **2** to form $[Fe^{III}(TMC)(\eta^1\text{-}OOH)]^{2+}$ (**5**) in CH_3CN,[7a] indicating partial neutralization of the negative charge of the peroxo ligand. Titration of **2** with $Sc(OTf)_3$ showed that 1 equiv of $Sc(OTf)_3$ was nearly sufficient to cause the 835 nm band of **2** to disappear, suggesting a 1:1 stoichiometry for the Sc^{3+} adduct of **2** (Figure 2B). The EPR spectrum of **3** shows features at g = 9.1, 5.1, 3.6, and ∼2, consistent with an $S = {}^5/_2$ Fe(III) center with an E/D ratio of 0.18 (Figure 3 left), compared with E/D = 0.28 and 0.097 for **2** and **5**,[7a] respectively. The Mössbauer spectra of **3** (Figure 3 right) are typical of high-spin Fe(III); their analysis is described in the SI, and the Mössbauer parameters are listed in Table 1 and the Figure 3 caption. A comparison of the spectroscopic properties in Table 1 shows that **3** is quite different from **2** and **5**, indicating that Sc^{3+} significantly affects the properties of the peroxoiron(III) unit.

We also carried out Fe K-edge X-ray absorption spectroscopy (XAS) studies to investigate the structural features of **3**. Complex **3** exhibited an Fe K-edge at 7125.3 eV and a pre-edge feature at 7113.3 eV, which are comparable to those of **2** and **5** obtained in CH_3CN (Figure S4 and Table S1).[7a] The pre-edge feature of **3** has an area of 14.4(6) units, compared with 17.9 for **2** and 22.4 for **5** (Table S1). As the pre-edge area reflects the extent to which the iron center deviates from centrosymmetry, the coordination environment of **3** must be

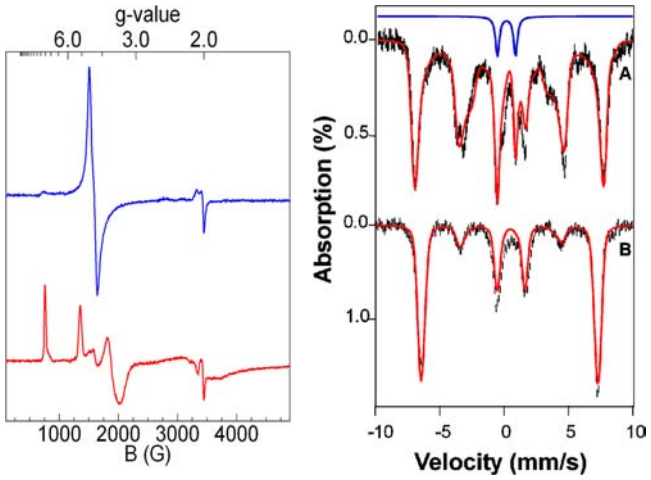

Figure 3. (left) EPR spectra of **2** (blue)[7a] and **3** (red) at 2 K and a microwave power of 0.2 mW. (right) Mössbauer spectra of **3** at 4.2 K in MeCN recorded in parallel applied fields of (A) 0.5 and (B) 8.0 T. The red lines in (A) and (B) are theoretical curves based on eq 1 in the SI using the following parameters: D = +1.3 cm^{-1}, E/D = 0.18, g_0 = 2.00, $A_x/g_n\beta_n$ = −20.0 T, $A_y/g_n\beta_n$ = −20.6 T, $A_z/g_n\beta_n$ = −19.9 T, ΔE_Q = 0.50 mm/s, η = −0.5, δ = 0.47 mm/s. The Mössbauer sample contained 90% **3**[8] and 10% Fe^{IV}=O species (blue line).

Table 1. Spectroscopic Comparison of Fe^{III}(TMC)−Peroxo Complexes ($S = {}^5/_2$) in CH_3CN

	λ_{max} (nm)	ΔE_Q (mm/s)	δ (mm/s)	D (cm^{-1})	E/D	pre-edge area	ref
2	835	−0.92	0.58	−0.91	0.28	17.9	7a
3	520	0.50	0.47	1.3	0.18	14.4	−[a]
5	500	0.20	0.51	2.5	0.097	22.4	7a

[a]This work.

closer to that of **2** with an η^2-peroxo ligand than that of **5** with an η^1-OOH ligand.

Analysis of the extended X-ray absorption fine structure (EXAFS) data for **3** provided additional structural insight. Best fits revealed four N scatterers at 2.18 Å and four C scatterers each at 3.00 and 3.15 Å (Figure 4 and Table S2); all of these features arise from the TMC ligand and have distances close to those found for **2** (Table 2). In addition, there is an O subshell at 1.98(1) Å arising from the peroxo ligand. Notably, the Fe−O distance (r_{Fe-O}) in **3** is significantly longer than the distance of 1.91 Å found for **2**,[7a] implying that the addition of Sc^{3+}

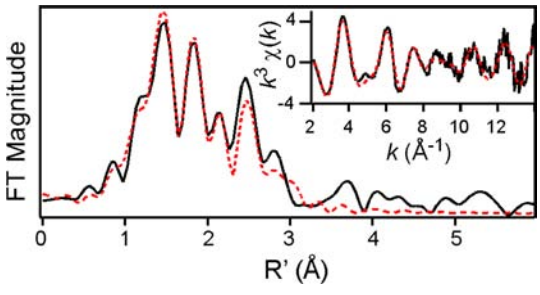

Figure 4. Fourier transform of the Fe K-edge EXAFS data for **3** over a k range of 2−14 $Å^{-1}$. The inset shows $k^3\chi(k)$ vs k data. The solid black lines represent the experimental data, while the red dashed lines correspond to the best fit with two O at 1.98 Å and four N at 2.18 Å (fit 22 in Table S3).

dx.doi.org/10.1021/ja402645y | J. Am. Chem. Soc. 2013, 135, 10198−10201

Table 2. Comparison of Structural and Raman Data for $S = {}^5/_2$ Fe^{III}–Peroxo Complexes

complex	r_{Fe-N} (Å)	r_{Fe-O} (Å)	ν_{O-O} (cm^{-1})	refs
3[a]	2.18	1.98, 1.98	807	–[b]
non-heme Fe^{III}–η^2-peroxo			816–827	7, 15
2 (**2′**)[a]	2.20 (2.21)	1.91, 1.91 (1.91, 1.91)	826 (825)	7a (7b)
non-heme Fe^{III}–η^1-peroxo			830–891	7, 16[c]
5 (**5′**)[a]	2.15 (2.16)	1.92 (1.85)	870 (868)	7a (7b)
6	2.17	1.89		17
(heme)Fe^{III}–(μ-η^2:η^1-O_2)–Cu^{II}	2.09	1.92, 2.09	788–808	9a, 9b
(heme)Fe^{III}–(μ-η^2:η^2-O_2)–Cu^{II}	2.09	1.94, 2.09	747–767	9a, 9b

[a]**2**, **3**, and **5** in CH_3CN; **2′** and **5′** in 3:1 (v/v) acetone/CF_3CH_2OH. [b]This work. [c]Also see Table S4 in the SI of ref 7a.

significantly weakens the iron–peroxo interaction. This 0.07 Å lengthening is inconsistent with conversion of the η^2-peroxo ligand to an η^1 isomer, as the related η^1-peroxo complexes **5** and [Fe^{III}(TMCS)(η^1-O_2)] (**6**) [TMCS = 1-(2-mercaptoethyl)-4,8,11-trimethyl-1,4,8,11-tetraazacyclotetradecane] have shorter Fe–O distances (Table 2). Cu^{II} adducts to (η^2-peroxo)iron(III) porphyrin complexes also have one short Fe–O bond (~1.93 Å) in a highly unsymmetric η^2-peroxo ligand that binds to the iron.[9] Thus, the 0.07 Å lengthening of r_{Fe-O} in **3** relative to that in **2** favors a symmetric η^2-peroxo binding mode for **3**. This conclusion is also supported by a comparison of fits 7 and 8 in Table S2, where the two-O subshell in fit 7 has a σ^2 value of ~4, while the one-O subshell in fit 8 has a σ^2 value of −0.4. The negative σ^2 value for the latter indicates that either a bond is more rigid than would be expected for its distance or that there are too few scatterers associated with that shell.[10] A negative σ^2 value was also found when only one O scatterer (instead of two) was used in fitting the EXAFS data for **2**. Our EXAFS results thus demonstrate that the binding of Sc^{3+} retains the symmetric side-on binding mode of the peroxo ligand in **3** but increases r_{Fe-O} by 0.07 Å.[11]

The final key piece of evidence for the identity of **3** was provided by resonance Raman spectroscopy. Laser excitation into the intense 520 nm band of **3** revealed two prominent peaks at 807 and 543 cm^{-1} (Figure 5) that correspond to ν_{O-O} and ν_{Fe-O} modes, respectively. These assignments were corroborated by ^{18}O labeling, which resulted in respective downshifts of 45 and 23 cm^{-1} that correlate well with Hooke's Law predictions for these modes and support the presence of an iron-bound peroxo ligand in **3**. The ν_{O-O} of **3** is the lowest of any non-heme high-spin peroxoiron(III) complex observed to date (Table 2). Relative to its precursor **2**,[7a] **3** has a ν_{O-O} that is downshifted by 19 cm^{-1} and a ν_{Fe-O} that is upshifted by 50 cm^{-1},[12] consistent with retention of the η^2 binding mode of the peroxo ligand. Taken together, the spectrosopic data lead us to propose an Fe^{3+}–(μ-η^2:η^2-O_2)–Sc^{3+} core for **3**, analogous to the Ni^{2+}–(μ-η^2:η^2-O_2)–K^+ core found in a complex characterized crystallographically by Limberg, Driess, and co-workers.[13,14]

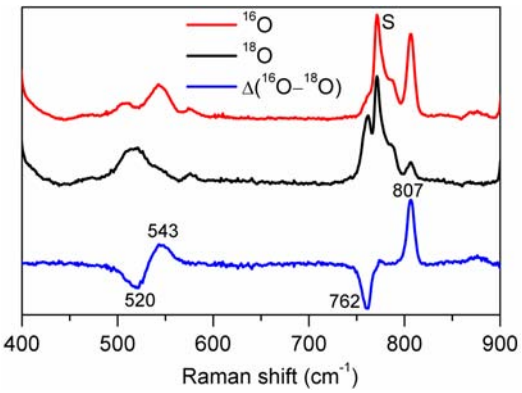

Figure 5. Resonance Raman spectra of **3** prepared in CH_3CN with $H_2{}^{16}O_2$ (red) and $H_2{}^{18}O_2$ (black) obtained with 514.5 nm excitation at 100 mW. The ^{16}O – ^{18}O difference spectrum is shown in blue. S = solvent-derived peaks.

With the nature of **3** characterized, an important question that remains is whether **3** is involved in the conversion of **1** to **4** by O_2 activation. The requirement for both Sc^{3+} and two electrons to trigger O_2 activation of **1** suggests the likely formation of a Sc^{3+}–peroxo–Fe^{3+} species such as **3** as an intermediate (Scheme 1). However, the fact that this species did not accumulate during O_2 activation (Figure 1A) suggests that **3** may correspond to a more stable isomer of the actual intermediate involved in the O_2 activation reaction. Nevertheless, **3** represents a rare example of a heterobimetallic complex bridged by a peroxo ligand[9,13] and the only one to date that involves a non-heme iron center.

The spectroscopic characterization of **3** as a complex with an Fe^{3+}–(μ-η^2:η^2-O_2)–Sc^{3+} core provides a plausible mechanism for a Lewis acid to promote O–O bond cleavage. This insight points to another role the second iron center can play in diiron enzymes besides serving as an electron source: functioning as a Lewis acid to facilitate the formation of high-valent iron–oxo intermediates such as **Q** and **X** in the respective oxygen activating cycles of methane monooxygenase and class 1A ribonucleotide reductases.[18] This report of the Sc^{3+}–peroxo–Fe^{3+} intermediate **3** also augments the recent literature focused on the effects of redox-inactive Lewis acidic metal ions on redox transformations.[1−3] Prominent among these are their accelerative properties in oxidations by high-valent metal–oxo complexes discovered by Fukuzumi and Nam[2a−f] as well as the role of Ca^{2+} in forming an O–O bond from water during photosynthesis.[1] Relevant to the latter, Borovik recently showed that group-II metal ions (M^{II}) can enhance the rates of O_2 activation by Fe^{II} and Mn^{II} complexes to afford well-characterized M^{II}–(μ-OH)–(Mn^{III}/Fe^{III}) products, presumably via heterobimetallic O_2 adducts.[3] The present results demonstrate that Sc^{3+} can "turn on" the activation of O_2 at a non-heme iron center *and* that a transient Sc^{3+}–peroxo–Fe^{3+} species related to **3** could be a viable intermediate leading to O–O bond cleavage.

■ ASSOCIATED CONTENT

Supporting Information

Syntheses; physical methods; ESI-MS, ^1H NMR, and XANES figures; and details of XAS analyses. This material is available free of charge via the Internet at http://pubs.acs.org.

dx.doi.org/10.1021/ja402645y | J. Am. Chem. Soc. 2013, 135, 10198–10201

AUTHOR INFORMATION

Corresponding Author

emunck@cmu.edu; larryque@umn.edu

Present Addresses

[§]F.L.: Brookhaven National Laboratory, Upton, NY 11973.
[‖]K.M.V.H.: Harvey Mudd College, Claremont, CA 91711.

Notes

The authors declare no competing financial interest.

ACKNOWLEDGMENTS

This work was supported by the National Science Foundation (Grant CHE1058248 to L.Q.) and the National Institutes of Health (Grant EB001475 to E.M. and postdoctoral fellowship GM093479 to K.M.V.H.). F.L. acknowledges a doctoral dissertation fellowship from the University of Minnesota. XAS data were collected at beamline X3B of the National Synchrotron Light Source at the Brookhaven National Laboratory and beamline 7-3 of the Stanford Synchrotron Radiation Lightsource, both supported by NIH and DOE. We thank Dr. Jason England and Ms. Jennifer Bigelow for assistance and discussions.

REFERENCES

(1) (a) Yocum, C. F. *Coord. Chem. Rev.* **2008**, *252*, 296. (b) Umena, Y.; Kawakami, K.; Shen, J.-R.; Kamiya, N. *Nature* **2011**, *473*, 55. (c) Tsui, E. Y.; Tran, R.; Yano, J.; Agapie, T. *Nat. Chem.* **2013**, *5*, 293.

(2) (a) Fukuzumi, S. *Coord. Chem. Rev.* **2013**, *257*, 1564. (b) Fukuzumi, S.; Morimoto, Y.; Kotani, H.; Naumov, P.; Lee, Y.-M.; Nam, W. *Nat. Chem.* **2010**, *2*, 756. (c) Morimoto, Y.; Kotani, H.; Park, J.; Lee, Y.-M.; Nam, W.; Fukuzumi, S. *J. Am. Chem. Soc.* **2011**, *133*, 403. (d) Park, J.; Morimoto, Y.; Lee, Y.-M.; Nam, W.; Fukuzumi, S. *J. Am. Chem. Soc.* **2011**, *133*, 5236. (e) Morimoto, Y.; Kotani, H.; Park, J.; Lee, Y.-M.; Nam, W.; Fukuzumi, S. *J. Am. Chem. Soc.* **2011**, *133*, 403. (f) Chen, J.; Lee, Y.-M.; Davis, K. M.; Wu, X.; Seo, M. S.; Cho, K.-B.; Yoon, H.; Park, Y. J.; Fukuzumi, S.; Pushkar, Y. N.; Nam, W. *J. Am. Chem. Soc.* **2013**, *135*, 6388. (g) Leeladee, P.; Baglia, R. A.; Prokop, K. A.; Latifi, R.; de Visser, S. P.; Goldberg, D. P. *J. Am. Chem. Soc.* **2012**, *134*, 10397.

(3) (a) Park, Y. J.; Ziller, J. W.; Borovik, A. S. *J. Am. Chem. Soc.* **2011**, *133*, 9258. (b) Park, Y. J.; Cook, S. A.; Sickerman, N. S.; Sano, Y.; Ziller, J. W.; Borovik, A. S. *Chem. Sci.* **2013**, *4*, 717.

(4) Thibon, A.; England, J.; Martinho, M.; Young, V. G., Jr.; Frisch, J. R.; Guillot, R.; Girerd, J.-J.; Münck, E.; Que, L., Jr.; Banse, F. *Angew. Chem., Int. Ed.* **2008**, *47*, 7064.

(5) Rohde, J.-U.; In, J.-H.; Lim, M. H.; Brennessel, W. W.; Bukowski, M. R.; Stubna, A.; Münck, E.; Nam, W.; Que, L., Jr. *Science* **2003**, *299*, 1037.

(6) Likewise, no intermediates were observed in the previously reported reactions of **1** and O_2 to form **4**, irrespective of whether it was promoted by H^+/BPh_4^-,[4] NADH analogues (see: Hong, S.; Lee, Y.-M.; Shin, W.; Fukuzumi, S.; Nam, W. *J. Am. Chem. Soc.* **2009**, *131*, 13910.), or cycloalkene (see: Lee, Y.-M.; Hong, S.; Morimoto, Y.; Shin, W.; Fukuzumi, S.; Nam, W. *J. Am. Chem. Soc.* **2010**, *132*, 10668).

(7) (a) Li, F.; Meier, K. K.; Cranswick, M. A.; Chakrabarti, M.; Van Heuvelen, K. M.; Münck, E.; Que, L., Jr. *J. Am. Chem. Soc.* **2011**, *133*, 7256. (b) Cho, J.; Jeon, S.; Wilson, S. A.; Liu, L. V.; Kang, E. A.; Braymer, J. J.; Lim, M. H.; Hedman, B.; Hodgson, K. O.; Valentine, J. S.; Solomon, E. I.; Nam, W. *Nature* **2011**, *478*, 502. (c) Liu, L. V.; Hong, S.; Cho, J.; Nam, W.; Solomon, E. I. *J. Am. Chem. Soc.* **2013**, *135*, 3286.

(8) We had difficulties obtaining simulations that simultaneously fit the 0.5 and 8.0 T spectra. We suspect that the Hamiltonian requires the introduction of quartic terms, as we found previously for **2**.[7a]

(9) (a) Halime, Z.; Kieber-Emmons, M. T.; Qayyum, M. F.; Mondal, B.; Gandhi, T.; Puiu, S. C.; Chufán, E. E.; Sarjeant, A. A. N.; Hodgson, K. O.; Hedman, B.; Solomon, E. I.; Karlin, K. D. *Inorg. Chem.* **2010**, *49*, 3629. (b) Chufán, E. E.; Puiu, S. C.; Karlin, K. D. *Acc. Chem. Res.* **2007**, *40*, 563. (c) Chishiro, T.; Shimazaki, Y.; Tani, F.; Tachi, Y.; Naruta, Y.; Karasawa, S.; Hayami, S.; Maeda, Y. *Angew. Chem., Int. Ed.* **2003**, *42*, 2788.

(10) Scott, R. A. In *Physical Methods in Bioinorganic Chemistry: Spectroscopy and Magnetism*; Que, L., Jr., Ed.; University Science Books: Sausalito, CA, 2000; pp 465−503.

(11) We attempted to include in fits of **3** a Sc scatterer at ∼3.7 Å. Fits 13 and 14 in Table S2 show that a Sc scatterer at 3.8 Å with a reasonable Debye−Waller factor ($\sigma^2 \approx 4$) could be added but gave only a slight improvement in the goodness of fit. Similar results were obtained in the EXAFS analysis of a Sc−O−Co complex (see: Pfaff, F. F.; Kundu, S.; Risch, M.; Pandian, S.; Heims, F.; Pryjomska-Ray, I.; Haack, P.; Metzinger, R.; Bill, E.; Dau, H.; Comba, P.; Ray, K. *Angew. Chem., Int. Ed.* **2011**, *50*, 1711).

(12) At first glance, the 50 cm^{-1} upshift in the Fe−O vibration in going from **2** to **3** may appear to contradict the observed lengthening of the Fe−O bond distance deduced from the EXAFS analysis, but the ^{18}O shifts found for the respective Fe−O vibrations were quite different (−15 vs −23 cm^{-1}). The downshift for **3** is as calculated for a diatomic Fe−O oscillator, but the smaller shift for **2** indicates mixing of the diatomic Fe−O vibration with other vibrational modes. Thus, the use of a direct comparison of the frequencies to deduce the Fe−O bond distance is not valid in this case.

(13) Yao, S.; Xiong, Y.; Vogt, M.; Grützmacher, H.; Herwig, C.; Limberg, C.; Driess, M. *Angew. Chem., Int. Ed.* **2009**, *48*, 8107.

(14) A related $Fe^{3+}-(\mu\text{-}\eta^2\text{:}\eta^2\text{-}O_2)-H^+$ core was postulated by Nam for a short-lived (<2 ms) species (λ_{max} = 527 nm) observed at −40 °C upon treatment of **2** with strong acid in its conversion to **5**.[7b]

(15) (a) Girerd, J.-J.; Banse, F.; Simaan, A. J. *Struct. Bonding* **2000**, *97*, 145. (b) Roelfes, G.; Vrajmasu, V.; Chen, K.; Ho, R. Y. N.; Rohde, J.-U.; Zondervan, C.; la Crois, R. M.; Schudde, E. P.; Lutz, M.; Spek, A. L.; Hage, R.; Feringa, B. L.; Münck, E.; Que, L., Jr. *Inorg. Chem.* **2003**, *42*, 2639. (c) Simaan, A. J.; Döpner, S.; Banse, F.; Bourcier, S.; Bouchoux, G.; Boussac, A.; Hildebrandt, P.; Girerd, J.-J. *Eur. J. Inorg. Chem.* **2000**, 1627. (d) Neese, F.; Solomon, E. I. *J. Am. Chem. Soc.* **1998**, *120*, 12829.

(16) (a) Brunold, T. C.; Solomon, E. I. *J. Am. Chem. Soc.* **1999**, *121*, 8288. (b) Wada, A.; Ogo, S.; Nagatomo, S.; Kitagawa, T.; Watanabe, Y.; Jitsukawa, K.; Masuda, H. *Inorg. Chem.* **2002**, *41*, 616. (c) Kitagawa, T.; Dey, A.; Lugo-Mas, P.; Benedict, J. B.; Kaminsky, W.; Solomon, E.; Kovacs, J. A. *J. Am. Chem. Soc.* **2006**, *128*, 14448. (d) Katona, G.; Carpentier, P.; Nivière, V.; Amara, P.; Adam, V.; Ohana, J.; Tsanov, N.; Bourgeois, D. *Science* **2007**, *316*, 449.

(17) McDonald, A. R.; Van Heuvelen, K. M.; Guo, Y.; Li, F.; Bominaar, E. L.; Münck, E.; Que, L., Jr. *Angew. Chem., Int. Ed.* **2012**, *51*, 9132.

(18) (a) Tinberg, C. E.; Lippard, S. J. *Acc. Chem. Res.* **2011**, *44*, 280. (b) Stubbe, J.; Nocera, D. G.; Yee, C. S.; Chang, M. C. Y. *Chem. Rev.* **2003**, *103*, 2167.